Available online at www.sciencedirect.com
ScienceDirect
Catalysis Today 120 (2007) 158–162
CATALYSIS TODAY
www.elsevier.com/locate/cattod

Photocatalytic partial oxidation of α-methylstyrene over TiO_2 supported on zeolites

Hidenori Yahiro *, Takaaki Miyamoto, Nobuyoshi Watanabe, Hiroyuki Yamaura

Department of Materials Science and Biotechnology, Graduate School of Science and Engineering, Ehime University, Matsuyama 790-8577, Japan

Available online 24 August 2006

Abstract

The photocatalytic reaction in the partial oxidation of α-methylstyrene (α-MS) to acetophenone (AP) was investigated for TiO_2 supported on Y-type, moredenite, and ZSM-5 zeolites. XRD and FT-Raman results demonstrated that the anatase is the stable phase of TiO_2 supported on zeolites and no rutile phase was observed in the supported catalysts calcined at 723–973 K. TiO_2 supported on zeolites was found to catalyze the partial oxidation of α-MS to AP under light irradiation (>290 nm). The photocatalytic activity of TiO_2 supported on zeolites was significantly improved by the addition of the water to the organic solvent. It was found that the optimized amount of water added for TiO_2 supported on zeolite catalysts was smaller than that for TiO_2 catalyst.

Keywords: Titanium oxide; Zeolite; Photocatalyst; Oxidation; Styrene; Water addition

1. Introduction

Heterogeneous photocatalytic reaction of organic compounds over TiO_2 is attracting much attention as one of the economical energy system. In the environmental point of view, photocatalytic oxidation of organic substances has emerged for taking care of harmful organic pollutants in air or water. Among the semiconductive photocatalysts, TiO_2 has reported to be particularly active for the oxidation reaction because it possesses high oxidizing power [1–4].

Supported TiO_2 is often reported to be less photoactive due to the interaction of TiO_2 with support [5]. In some cases, however, the use of supports improved photocatalytic performances [6–17]. For example, Xu and Langford [9,11] have reported the photocatalytic degradation of acetophenone with TiO_2 supported on inorganic porous materials such as MCM-41, zeolite X, and zeolite Y. The positive effect for the supported TiO_2 catalysts was considered to be due to the increase in the adsorption of organic substances onto the support.

Apart from the photocatalytic oxidation of organic pollutants to less harmful compounds, partial oxidation of organic substrates is also an important process for providing chemicals as the industrial starting materials [18–20]. Recently, Ohno et al. [21] have found that the addition of water to organic solvent promoted the catalytic activity of TiO_2 for the partial oxidation of methylpyridine isomers. In this paper, we report the photocatalytic partial oxidation of α-methylstyrene (α-MS) to acetophenone (AP) over TiO_2 supported on zeolite under the condition with added water.

2. Experimental

2.1. Materials and instruments

TiO_2 powder containing both anatase and rutile phases was obtained from the Catalysis Society of Japan (JRC-TIO4). The zeolite supports, Na-ZSM-5 (abbreviated as MFI, SiO_2/Al_2O_3 = 23.8), Na-mordenite (MOR, 15.4), and Na-Y (FAU, 5.5), were obtained from the Tosoh Co. All chemicals, isopropanol (Wako, 99.5%), titanium(IV) tetraisopropoxide (Aldrich, 97%), α-MS (Aldrich, 99%), and acetonitrile (Wako, 99.5%), were used as received.

Zeolite-supported TiO_2 catalysts (designated as TiO_2/zeolite) were prepared by modifying the method reported by Xu and Langford [9]. The titanium(IV) tetraisopropoxide was added to the zeolite-suspended isopropanol solution and the

* Corresponding author. Tel.: +81 89 927 9929; fax: +81 89 927 9946.
E-mail address: hyahiro@eng.ehime-u.ac.jp (H. Yahiro).

0920-5861/$ – see front matter © 2006 Elsevier B.V. All rights reserved.
doi:10.1016/j.cattod.2006.07.039

mixture was stirred for 1 h. Water was added to the resulting slurry to hydrolyze titanium(IV) tetraisopropoxide adsorbed on zeolite. After filtration, the resulting cake was dried at 363 K overnight and calcined at 573–973 K for 3 h to yield TiO_2 supported on zeolites. The TiO_2 loading was unified to be 25 wt% for TiO_2/zeolite catalysts.

Powder XRD patterns of the catalysts were collected on a Rigaku RINT2200HF diffractometer using Cu Kα radiation. UV–vis, IR, and Raman spectra were recorded with a Hitachi U-4000, a Perkin-Elmer Spectrum One, and a JASCO RFT-800 spectrometers, respectively. The composition profiles near the surface of samples were analyzed by auger electron spectroscopy (AES, Perkin-Elmer Phi 650).

2.2. Photocatalytic reaction

The photocatalytic reactions were carried out in a cylindrical Pyrex glass cell (28 mm in diameter and 200 mm in height). In the present study, acetonitrile was used as a solvent because this solvent was reported to be relatively inert to self-oxidation [22]. The sample based on the same metal equivalence as 0.0125 g TiO_2 was suspended in 0.3 mL of α-MS, $(49.7 - x)$ mL of acetonitrile, and x mL of H_2O $(0 < x < 10)$ in the cylindrical Pyrex glass cell. After evacuating the glass cell for 5 min and subsequently bubbling of oxygen for 15 min, the suspended solution under oxygen atmosphere was irradiated with a 100 W high-pressure mercury lamp (wavelength $\lambda > 290$ nm) surrounded by cooling water circulation, while stirred magnetically. The catalysts and solution were separated by filtration and then the resulting solution was analyzed by GC–MS (Shimadzu GCMS-QP 5050A). The amounts of the organic compounds were determined by comparison with that of benzaldehyde (Wako, 98%) as an internal standard. The photocatalytic activity was evaluated by the yield of AP produced.

3. Results and discussion

3.1. Characterization of TiO_2 supported on zeolites

In order to confirm the crystalline structure of TiO_2/zeolite catalysts, XRD and FT-Raman studies were carried out. Fig. 1 shows the XRD patterns of TiO_2/MOR catalysts calcined at different temperatures. The XRD pattern of TiO_2/MOR catalyst calcined at 573 K (Fig. 1(b)) was essentially the same as that of the original MOR zeolite (Fig. 1(a)). When the TiO_2/MOR catalyst was calcined at higher temperatures, the XRD patterns of TiO_2/MOR catalysts were complicated because of the overlapping of diffraction peaks attributed to TiO_2 and those of the MOR support. As can be seen in Fig. 1(c and d), the peak assigned to an anatase phase was observed at $2\theta = 25.1^\circ$ for the TiO_2/MOR catalysts calcined at 723 and 973 K. The intensity of this peak increased when the samples were calcined at higher temperature, suggesting that the crystallinity of anatase increased with the calcination temperature. On the other hand,

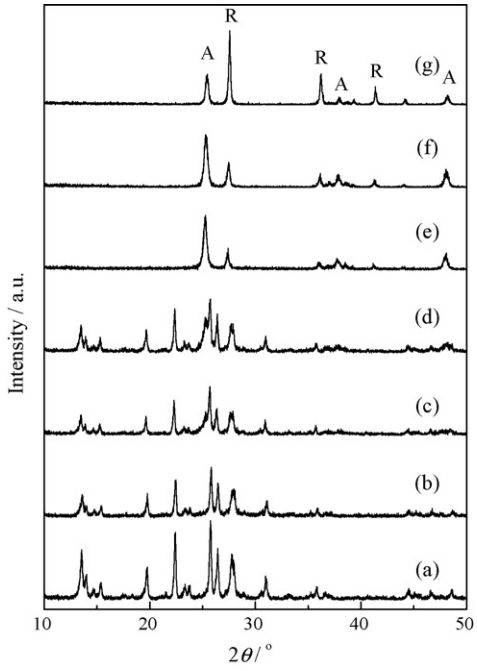

Fig. 1. XRD patterns of: (a) MOR, TiO_2/MOR calcined at (b) 523 K, (c) 723 K, and (d) 973 K for 3 h, (e) TiO_2, and TiO_2 calcined at (f) 723 K and (g) 973 K for 3 h.

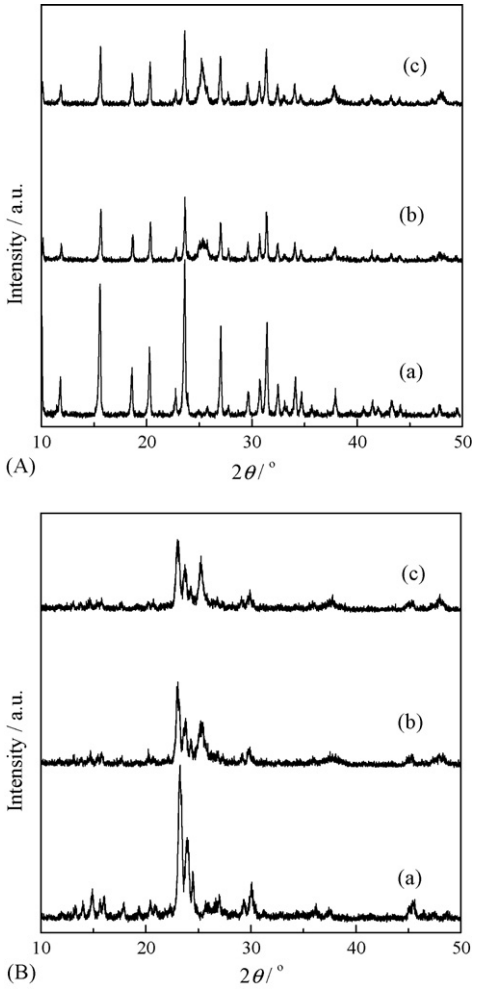

Fig. 2. XRD patterns of: (A-a) FAU and TiO_2/FAU calcined at (A-b) 723 K and (A-c) 973 K for 3 h and (B-a) MFI and TiO_2/MFI calcined at (B-b) 723 K and (B-c) 973 K for 3 h.

no peak assigned to rutile phase was observed in the XRD patterns of TiO_2/MOR catalysts calcined at 723–973 K. This result indicated that for the TiO_2/MOR catalysts, the anatase was the stable phase, being confirmed by FT-Raman spectra, as mentioned later. Fig. 1 also shows the XRD patterns of TiO_2 calcined at 723 and 973 K. The anatase (represented by 'A' in Fig. 1) was the main constituent for TiO_2 calcined below 723 K, but small amount of rutile (represented by 'R' in Fig. 1) was present. In contrast to TiO_2/MOR catalysts, the peak area of anatase decreased with an increase in calcination temperature, and simultaneously that of rutile increased.

Fig. 2 shows the XRD patterns of supported TiO_2 with different zeolite structures. The change in XRD patterns for TiO_2/MFI and TiO_2/FAU catalysts were similar to that for TiO_2/MOR catalyst; the anatase was the stable phase of TiO_2 and no rutile phase was observed in the supported catalysts calcined at 723–973 K.

FT-Raman spectra of TiO_2/zeolite and TiO_2 catalysts calcined at 723 and 973 K are shown in Fig. 3(A and B), respectively. FT-Raman spectrum of TiO_2 calcined at 723 K (Fig. 3(A-a) provided a series of the intense peaks at 640, 518, and 398 cm^{-1} assigned to anatase phase (represented by 'A' in Fig. 3) and a series of weak peaks at 613 and 447 cm^{-1} attributed to rutile phase (represented by 'R' in Fig. 3) [9,16,23]. The peaks due to anatase decreased slightly at higher calcination temperature and those due to rutile intensified (Fig. 3(B-a)). On the other hand, the FT-Raman spectra of TiO_2/FAU, TiO_2/MOR, and TiO_2/MFI calcined at 723 and 973 K confirmed that TiO_2 formed was in the anatase structure. The results of FT-Raman were consistent with XRD results.

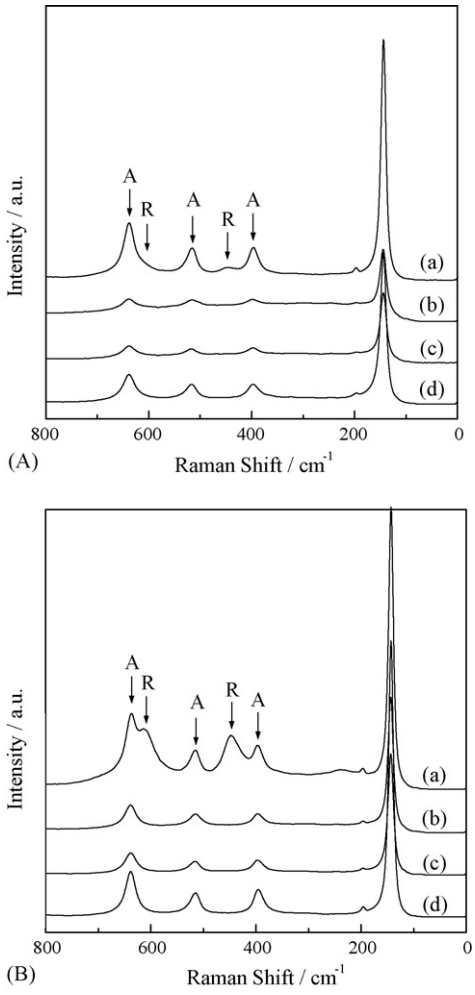

Fig. 3. FT-Raman spectra of: (a) TiO_2, (b) TiO_2/FAU, (c) TiO_2/MOR, and (d) TiO_2/MFI calcined at (A) 723 K and (B) 973 K for 3 h.

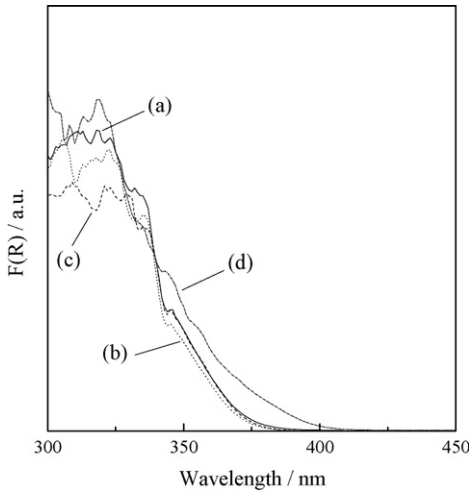

Fig. 4. UV–vis spectra of: (a) TiO_2/FAU, (b) TiO_2/MOR, (c) TiO_2/MFI, and (d) TiO_2 calcined at 723 K for 3 h.

The results from both XRD and FT-Raman indicate that TiO_2/zeolite catalysts, calcined at 723 and 973 K, were in the anatase form, independent of the zeolite structure, and that the zeolite structure remained unchanged even after heat treatment at 973 K. Xu and Langford [9] have reported that the noncrystalline TiO_2 was formed for TiO_2 supported on ZSM-5 and zeolite A, which was calcined at 723 K, besides anatase phase. We have no evidence concerning the formation of noncrystalline TiO_2; however, the fact that the XRD peak intensity originated from the anatase phase increased with increasing calcination temperature may support the presence of noncryatalline TiO_2 in supported samples calcined at 723 K.

Fig. 4 shows the UV–vis spectra of TiO_2/zeolite and TiO_2 catalysts. The absorption edge of TiO_2/zeolite was lower in wavelength than that of TiO_2. The absorption edge of an UV–vis spectrum corresponds to the band-gap energy of semiconductor and the band-gap energy can be evaluated by a plot of $[F(R_\infty)h\nu]^2$ as a function of $h\nu$ [24]. The calculated band-gap energies were 3.5 and 3.2 eV for TiO_2/zeolite and bare TiO_2, respectively. This suggests that the particle size of TiO_2 supported on zeolites is smaller than that of TiO_2 used in the present study (quantum size effect). Interestingly, the wavelength of the absorption edge was independent on the zeolite structure, whereas the pore size of each zeolite was different from each other. Considering the observation from the XRD diffraction peaks for the TiO_2/zeolite catalysts, the TiO_2 particles were presumed to be formed mainly on the outer surface of zeolites. This hypothesis was confirmed by AES analysis near the surface of samples. Fig. 5 shows the AES spectra of TiO_2/MFI and MFI samples calcined at 723 K for

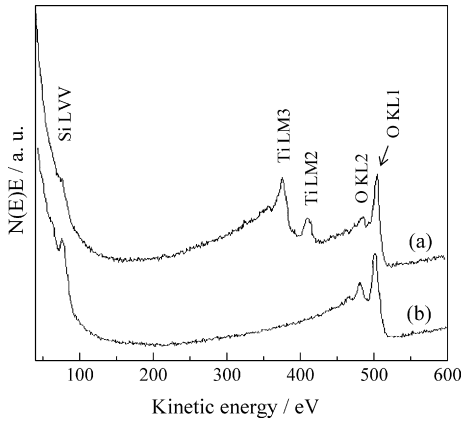

Fig. 5. AES analysis of: (a) TiO_2/MFI and (b) MFI catalysts calcined at 723 K for 3 h.

3 h. For AES spectrum of the TiO_2/MFI catalyst (Fig. 5(a)), two peaks assigned to Ti (kinetic energy = 375 and 408 eV) were clearly observed with those due to Si (75 eV) and O (470 and 500 eV) [25], indicating that titanium atoms were located near the surface of TiO_2/MFI catalyst. It should be noted that the intensity of AES peak originated from Si atoms for TiO_2/MFI catalyst was weaker than that for MFI zeolite (Fig. 5(b)). This implies that TiO_2 particles formed on the outside of MFI zeolite prevent to detect the Si atoms located near the zeolite surface.

3.2. Photocatalytic reaction

Beaune et al. [20] have previously reported that TiO_2 showed the activity towards the photo-oxidation of α-MS to AP. On the other hand, several studies have also shown the effect of water addition on the photocatalytic reaction of organic compounds over TiO_2 catalysts. In particular, Matsumura and co-workers [26] demonstrated that the presence of water is essential for the photohydroxylation of naphthalene as well as that of molecular oxygen. Therefore, it is conceivable that one should investigate the influence of the water addition on the catalytic activity of the photo-oxidation of α-MS over TiO_2/zeolite with different zeolite structure.

Fig. 6 shows the time course of the photocatalytic reaction over TiO_2/FAU, TiO_2/MOR, TiO_2/MFI, and TiO_2 catalysts calcined at 723 K. The activity monotonously increased with increasing irradiation time. The partial oxidation of α-MS over TiO_2/zeolite and TiO_2 was negligible without the light irradiation. For all the catalysts, AP was produced as the main product, as previously reported [20]. This result indicates that the cleavage of the carbon–carbon double bond to the corresponding carbonyl compounds occurs on catalysts. Besides AP, 2-phenylpropanaldehyde and polymer derived from α-MS were identified as by-products although no quantitative analysis of these by-products was carried out. The molar ratio of AP produced by the photocatalytic reaction during 24 h for TiO_2 supported on zeolites was ca. 4, indicating that the present reaction proceeds catalytically.

The result of the blank experiment without catalyst is also shown in Fig. 6. The yields of AP were <1 and 8% for 24 and 48 h, respectively, indicating that the direct photolysis of α-MS to AP occurred under the present light irradiation although the yield of AP without catalyst was smaller than those with supported TiO_2 catalysts. The yields of AP for MFI zeolite without TiO_2 loading were comparable to those without catalyst. This demonstrates that MFI zeolite is inert for photocatalytic reaction and the main reaction proceeds over TiO_2.

The catalytic activity depended on the calcination temperature of the catalysts, as shown in Fig. 7. The maximal activity was obtained at 723–823 K of calcination temperature. Considering XRD results shown in Fig. 1, the low activity of TiO_2/zeolite calcined at 573 K may result from less crystallinity of TiO_2, while the low activity of TiO_2/zeolite calcined at 973 K may result from the decrease in the surface area by the aggregation of TiO_2.

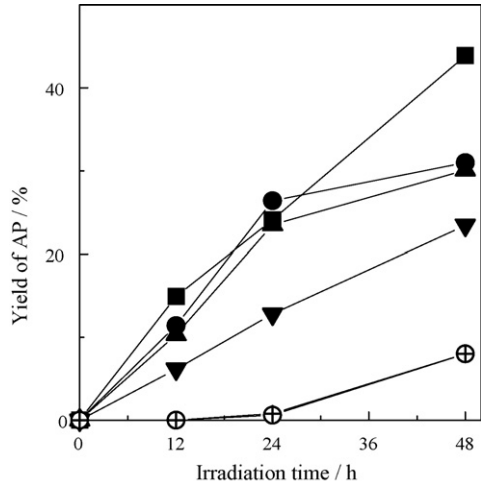

Fig. 6. The photocatalytic activities of: TiO_2/FAU (●), TiO_2/MOR (■), TiO_2/MFI (▲), TiO_2 (▼), and MFI (○) calcined at 723 K for 3 h as a function of the irradiation time. (+) Blank experiment without catalyst. *Reaction conditions*: α-MS (0.3 mL), H_2O (1.0 mL), and CH_3CN (48.7 mL).

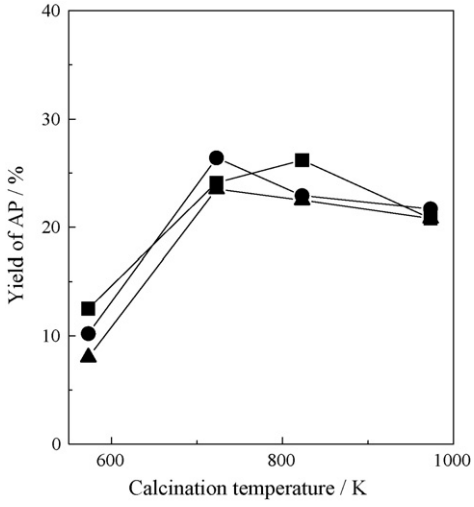

Fig. 7. The photocatalytic activities of: TiO_2/FAU (●), TiO_2/MOR (■) and TiO_2/MFI (▲) calcined at various temperatures for 3 h. *Reaction conditions*: α-MS (0.3 mL), H_2O (1.0 mL), CH_3CN (48.7 mL), and 24 h.

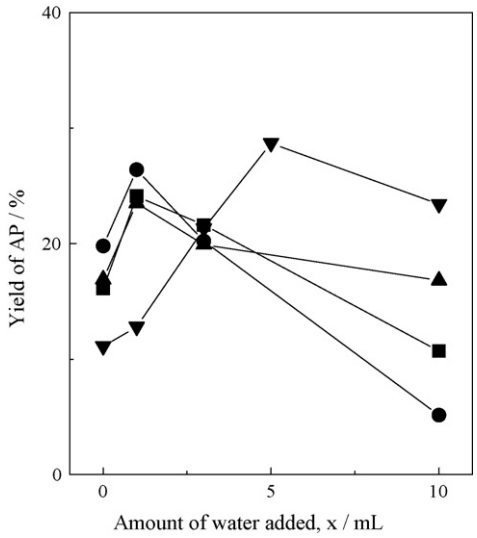

Fig. 8. The photocatalytic activities of: TiO_2/FAU (●), TiO_2/MOR (■), TiO_2/MFI (▲), and TiO_2 (▼) calcined at 723K for 3 h as a function of the amount of water added, *x*. *Reaction conditions*: α-MS (0.3 mL), CH_3CN (49.7 − *x*) mL, and 24 h.

Fig. 8 shows the activity of the TiO_2/zeolite catalysts as a function of the amount of water added to the solvent. The reaction time was 24 h and the samples were calcined at 723 K. The activity of TiO_2 calcined at 723 K is also shown in this figure for comparison. The activity of TiO_2 increased with the amount of water added, reached a maximal value at 5 mL of water addition, and then decreased with the further addition of water. This result indicates the photo-oxidation of α-MS to AP over TiO_2 was enhanced by the addition of water, as reported previously for the photo-oxidation of methylpyridine isomers [21] and the photohydroxylation of naphthalene [24]. When TiO_2 was supported on zeolites, the dependency of water addition on the photocatalytic activity was largely changed. As can be seen in Fig. 8, the maximal activity of TiO_2/zeolite catalyst was achieved by the smaller amount of water addition compared to that of TiO_2. This result supports that the efficiency of H_2O utilization was largely improved by supporting TiO_2 on zeolites since zeolite possesses the high adsorption ability of water. On the other hand, the activity of TiO_2/zeolite catalyst was less dependent on the zeolite structure—this may be due to the formation of crystalline TiO_2 particles on the outer surface of zeolite, as previously mentioned.

Mori et al. [27] and Suga et al. [28] studied the photocatalytic oxygenation of α-MS with molecular oxygen in the presence of photosensitizers. They reported that α-MS radical cation generated by photoinduced electron transfer reacts with molecular oxygen to give the deoxitane radical cation and that the decomposition of the deoxitane radical cation to AP and formaldehyde was accelerated by the presence of water. If the photo-oxygenation of α-MS over TiO_2 proceeds by a similar mechanism, the combination of TiO_2 with zeolite may result in the acceleration of the decomposition of the deoxitane radical cation because of the high adsorption ability of water on zeolites. As an alternative possibility, the zeolite may stabilize the intermediate species formed from oxygen and water as the result of the reactions with photogenarated electrons and holes on the TiO_2 surface [26]. Further studies are in progress in order to elucidate the reaction mechanism.

4. Conclusion

The photocatalytic oxidation of α-MS to AP was investigated using TiO_2 supported on zeolites such as Y-type, mordenite, and ZSM-5. XRD, FT-Raman, UV–vis, and AES results showed that the TiO_2 supported on zeolites was in the anatase form and was formed on mainly the outer surface of zeolite. The TiO_2/zeolite catalysts can catalyze the partial oxidation of α-MS with the aid of molecular oxygen dissolved in the solvent under the light irradiation (>290 nm). The addition of the small amount of water to the solvent was very effective in enhancing the catalytic reaction of the partial oxidation on TiO_2/zeolite catalysts.

Acknowledgement

This work was supported in part by the Core Research for Evolutional Science and Technology (CREST) program of the Japan Science and Technology Agency (JST).

References

[1] J.-M. Herrmann, Catal. Today 53 (1999) 115.
[2] O.M. Alfano, D. Bahnemann, A.E. Cassano, R. Dillert, R. Goslich, Catal. Today 58 (2000) 199.
[3] M. Mohseni, A. David, Appl. Catal. B 46 (2003) 219.
[4] C. Belver, M.J. López-Muñoz, J.M. Coronado, J. Soria, Appl. Catal. B 46 (2003) 497.
[5] O. Legrini, E. Oliveros, A. Braun, Chem. Rev. 93 (1993) 671.
[6] H. Yoneyama, S. Haga, S. Yamanaka, J. Phys. Chem. 93 (1989) 4833.
[7] C. Minero, F. Catozzo, E. Pelizzetti, Langmuir 8 (1992) 481.
[8] N. Takeda, T. Torimoto, S. Sampath, S. Kuwabara, H. Yoneyama, J. Phys. Chem. 99 (1995) 9986.
[9] Y. Xu, C.H. Langford, J. Phys. Chem. 99 (1995) 11501.
[10] T. Torimoto, S. Ito, S. Kuwabara, H. Yoneyama, Environ. Sci. Technol. 30 (1996) 1275.
[11] Y. Xu, C.H. Langford, J. Phys. Chem. B 101 (1997) 3115.
[12] P.G. Smirniotis, L. Davydov, Catal. Rev. Sci. Eng. 41 (1999) 43.
[13] H. Chen, A. Matsumoto, N. Nishimiya, K. Tsutsumi, Colloids Surf. A 157 (1999) 295.
[14] H. Yoneyama, T. Torimoto, Catal. Today 58 (2000) 133.
[15] Y.-H. Hsien, C.-F. Chang, Y.-H. Chen, S. Cheng, Appl. Catal. B 31 (2001) 241.
[16] C. Ooka, H. Yoshida, K. Suzuki, T. Hattori, Chem. Lett. 32 (2003) 896.
[17] S. Anandan, M. Yoon, J. Photchem. Photobiol. C: Photochem. Rev. 4 (2003) 5.
[18] M.A. Fox, Top. Curr. Chem. 142 (1987) 71.
[19] T. Ohno, K. Nakabeya, M. Matsumura, J. Catal. 176 (1986) 76.
[20] O. Beaune, A. Finiels, P. Geneste, P. Graffin, J.-L. Olivé, A. Saaedan, J. Chem. Soc., Chem. Commun. (1992) 1649.
[21] T. Ohno, T. Tsubota, R. Inaba, J. Appl. Electorochem. 35 (2005) 783.
[22] Y.H. Lin, I.D. Williams, P. Li, Appl. Catal. A 150 (1997) 221.
[23] S.R. Dhage, V.D. Choube, V. Samuel, V. Rabi, Mater. Lett. 58 (2004) 2310.
[24] A. Karcally, I. Hevesi, Z. Naturforsch. A 26 (1971) 245.
[25] A. Gunhold, K. Gömann, L. Beuermann, V. Kempter, G. Borchardt, W.M. Friedrichs, Surf. Sci. 566–568 (2004) 105.
[26] J. Jia, T. Ohno, Y. Masaki, M. Matsumura, Chem. Lett. (1999) 963.
[27] T. Mori, M. Takamoto, Y. Take, J. Shinkuma, T. Wada, Y. Inoue, Tetrahedron Lett. 42 (2001) 2505.
[28] K. Suga, K. Ohkubo, S. Fukuzumi, J. Phys. Chem. 107 (2003) 4339.